Earthquakes and Structures, *Vol. 7, No. 3 (2014) 385-400*
DOI: http://dx.doi.org/10.12989/eas.2014.7.3.385

Influence of mass and contact surface on pounding response of RC structures

Sushil Khatiwada*, Tam Larkin and Nawawi Chouw

Department of Civil and Environmental Engineering, the University of Auckland, Auckland Mail Centre, Private Bag 92019, Auckland 1142, New Zealand

(Received April 3, 2014, Revised May 19, 2014, Accepted May 20, 2014)

Abstract. Pounding damage to bridges and buildings is observed in most major earthquakes. The damage mainly occurs in reinforced concrete slabs, e.g. building floors and bridge decks. This study presents the results from pounding of reinforced concrete slabs. A parametric investigation was conducted involving the mass of the pendulums, the relative velocities of impact and the geometry of the contact surface. The effect of these parameters on the coefficient of restitution and peak impact acceleration is shown. In contrast to predictions from numerical force models, it was observed that peak acceleration is independent of mass. The coefficient of restitution is affected by the impact velocity, total participating mass and the mass ratio of striker and struck block.

Keywords: structural pounding; contact surface; mass variation effect; coefficient of restitution; impact acceleration

1. Introduction

Seismic pounding has been observed during many past earthquakes e.g., Loma Prieta 1989 (Kasai and Maison 1997), Christchurch 2011 (Chouw and Hao 2012) and Bhuj 2001 (EERI report 2001). The most widespread pounding damage resulted from the Mexico City 1985 earthquake (Rosenblueth and Meli 1986) where complete collapse occurred. Pounding takes place when adjacent buildings have different dynamic properties and the separation gap is inadequate to cope with the relative closing motion. The relative motion can also be caused by foundation deformation (Chouw 2002) and spatial variation of ground motion (Athanassiadou *et al*. 1994, Chouw and Hao 2008). Pounding occur between adjacent bridge decks (Li *et al*. 2012) or between deck and abutment (Li *et al*. 2013). Because of its frequency pounding is recognized as an urban seismic hazard (Jeng and Tzeng 2000, Bothara *et al*. 2008, Cole *et al*. 2010) and many numerical and experimental studies can be found in the literature.

Van Mier *et al*. (1991) subjected a 20 m long, stationary concrete beam to a longitudinal, horizontal impact by a square concrete bar. The stationary beam was 250 × 250 mm in cross-section and partially fixed at the other end by a buffer. A parametric study was conducted by varying the mass, velocity and contact surface geometry. The mass was varied by using two

*Corresponding author, Ph.D. Student, E-mail: skha178@aucklanduni.ac.nz

http://www.techno-press.org/?journal=eas&subpage=7 ISSN: 2092-7614 (Print), 2092-7622 (Online)

different strikers, i.e. 700 × 600 × 600 mm resulting in 570 kg mass and 650 × 400 × 400 mm resulting in 290 kg mass. Two velocities 0.5 m/s and 2.5 m/s were considered. Three striker surfaces *i.e*. hemispherical, conical and plane surface and two beam contact surfaces *i.e*. plane and corrugated surfaces were used. For each specimen, repeated impacts were conducted until the striker's surface was extensively damaged. The force time history was obtained from the accelerometers attached to the mid-point of the beam. A peak value was observed in the force time history after which it remains constant until finally decaying. The rise time to the peak value and fall time from peak to zero was dependent upon the impact velocity, masses and contact surface geometries. Van Mier *et al*. calculated the stiffness of the hemispherical contact to be 44 $kN/mm^{3/2}$, which is significantly less than the theoretical value of 201.73 $kN/mm^{3/2}$ obtained from the Hertz contact law (oldsmith 2001, Muthukumar and DesRoches 2006).

An early work by Leibovich *et al*. (1994) involved conducting a shake table simulation of pounding between two RC slabs supported by steel frames. The coefficient of restitution, defined as the ratio of relative velocity just after impact to the relative velocity just before impact, was 0.35 for an impact velocity of 40 cm/s. However, it is not clear whether that coefficient of restitution was for concrete-concrete or concrete-timber-concrete pounding.

Papadrakakis and Mouzakis (1995) conducted a shake table simulation of pounding between two storey RC frames. The slabs of the stiffer frame had a rectangular protrusion at the midpoint facing the second frame. The sipounding simulation was conducted under a ramped sinusoidal motion with no separation between the frames. The frequency of ground excitation was equal to the fundamental frequency of the flexible building. The peak accelerations increased up to six-fold in both frames. The study also compared the experimental results with that obtained from Lagrange multiplier method of pounding simulation and concluded that the numerical simulation produced good agreement with the experimental solutions. However, the results diverged substantially toward the end of the time window considered in both pounding and non-pounding cases.

Jankowski (2010) measured the coefficient of restitution when spheres, made of steel, concrete timber and ceramic were dropped on a plane surface of the same material. For each material the impacts were repeated for seven different velocities for three different diameters. A cubic polynomial best represented the relationship between coefficient of restitution and impact velocity. The coefficient of restitution was found independent of the mass of the ball. For the same series of tests, Jankowski (2007) found that the contact stiffness of the nonlinear viscoelastic force model (Jankowski 2005) was independent of velocity but varied with the falling mass. These experiments do not pay due regard to the influence of the undefined target mass. Jankowski (2010) carried out a shake table simulation of pounding between two steel frames with the four types of contact interfaces i.e. concrete, steel, timber and ceramic. In comparison to experimental results, numerical simulations with impact velocity-dependent coefficient of restitution were slightly closer than those obtained using a constant coefficient of restitution. The constant coefficient of 0.65 is based from previous studies e.g. Anagnostopoulos (1988).

Guo *et al*. (2009) carried out a shake table investigation on pounding reduction of base-isolated highway bridges. The bridge decks were loaded with RC masses while the deck and the impact interface were made of steel. Previous numerical studies, e.g. Zhu *et al*. (2000) and Muthukumar and DesRoches (2006), assumed that the impact element stiffness of linear viscoelastic model is equal to the axial stiffness of the decks. However, Guo *et al*. found that the impact stiffness is about 100 times smaller than the axial stiffness.

Leibovich *et al*. (2012) measured coefficient of restitution and impact acceleration for plane-ended circular concrete rods suspended as pendulums. Two different cases (i) bars of equal (1000 mm) length and (ii) bars of unequal (1000 mm and 500 mm) were considered. The coefficients of restitution calculated were 0.5 to 0.7 for the pounding between equal bars. In contrast to numerical predictions, e.g. Malhotra (1998) and Cole *et al*. (2011), the coefficient of restitution is higher when the longer bar was hit by the shorter bar. The recorded acceleration also showed multiple peaks with subsequent oscillation around the zero value.

A shake table simulation of pounding between a base-isolated building against a moat-like wall was presented by Masroor and Mosqueda (2012b). The building was modelled by a steel frame. A concrete block was used as contact element with the surrounding wall. Two types of walls were used: (i) concrete with soil backfill and (ii) stiff steel plate without backfill. The wall substantially affected the characteristics of the impact force recorded by load cells placed between the concrete block and the mat foundation of the building. Numerical simulation by Masroor and Mosqueda (2012a) found that the contact force time history had two phases: (i) the impact phase where the contact force develops and (ii) the quasi-static passive-pressure phase between the wall and building. Thus, the impact force alone was not sufficient to separate the two structures.

The literature review above revealed an absence of experimental studies where both the pounding masses and the contact components are constructed of RC. In addition, no study on the effects of mass and contact surface geometry has been reported. This paper addresses the identified knowledge gap, i.e. the consequence of the mass of the pendulums, the relative velocities of impact and the geometry of the contact surface, for coefficient of restitution and peak impact acceleration. The experiment results are essential for validating numerical models for estimating the pounding force for structural seismic design.

2. Experimental setup

The experiment involved impact between two pendulums (Fig. 1). The pendulum was made of single or multiple concrete slabs of size 550 × 500 × 120 mm. To avoid damage to the slabs

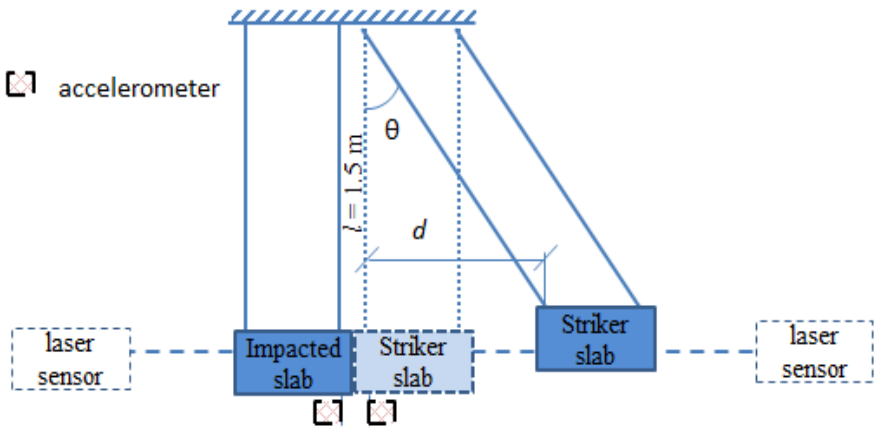

Fig. 1 Schematic drawing of the test setup

removable contact elements were used. All the contact elements had a base of size 550 × 100 × 120 mm. For all tests, the struck slab had a plane contact surface, and the striker slab had spherical, cylindrical or rectangular surface. Table 1 lists the geometries of the contact elements.

The impact tests for each mass combination were performed at eight different velocities. The acceleration and displacement of the slabs were measured.

2.1 Preparation of specimens

A design mix of cement: sand: 12.5 mm nominal aggregate of 1: 1.5: 3 respectively by volume was used. This is the nominal mix for M20 concrete recommended by IS:456 (Indian Bureau of Standards 2000). The moulds for the slabs and attachment are shown in Fig. 2. A steel reinforcement of 6 mm ϕ @ 120 mm c/c was used for each slab (Fig 3(a)). Six slabs and twenty contact elements were cast in ten different concrete batches. For each batch, three cylinder specimens were prepared and subjected to compression test after 28 days. The compressive strength of the cylinders was between 28 and 34 MPa.

(a) (b)

Fig. 3 Casting of (a) RC slab and (b) contact elements and cylinder specimens

(a) (b)

Fig. 1 Casting of (a) RC slab and (b) contact elements and cylinder specimens

Fig. 2 Contact elements

Table 1 Contact elements

Type	Size
Spherical	100 mm diameter
Cylindrical	100 mm diameter 150 mm length
Plane	150 mm length 100 mm width

The pounding elements were cast with soft wooden dowels (Fig. 4) of 12 mm diameter. These dowels were drilled out after curing was complete. A face of each slab was drilled and fitted with ϕ 12 mm anchor bolts to attach the pounding elements. Since the bolt heads would protrude and prevent contact for cylindrical and plane contact elements, a larger timber dowel was used near their face (see the bottom right contact element in Fig. 4). This large dowel extended 20 mm in the concrete. The bolt heads fit within these larger holes and thus contact between striker and struck surfaces is achieved.

2.2 Test setup and Instrumentation

The pendulums were constructed by suspending the concrete slabs from an overhead girder with four 6 mm ϕ steel cables (Fig. 5). The cables were fitted with turnbuckles for levelling and alignment. The cables were connected to a 50 × 50 × 6 mm angle at their lower end. Two angles are placed on the top of the slabs, and two on the bottom. Two 10 mm ϕ bolts were used to hold the slabs and the angles together. The length of the pendulum is considered to be the vertical distance between the fastener of the cable with the angles and the fastener at the overhead girder. For single slabs, this length is 1.5 m. The period of both pendulums matched that obtained from theoretical formula, $T = 2\pi\sqrt{l/g}$ for small angular displacements i.e. $\theta << 1$. A total of nine mass combinations (Table 2) were considered. Each pendulum in Fig. 5 has three slabs to illustrate the heaviest case. The additional slabs in the double and triple slab cases were inserted between the top angle and impacting slab. Since impact occurs at the mid-thickness of the bottom slabs, the line of action of the pounding force does not pass through the centre of mass in double and triple

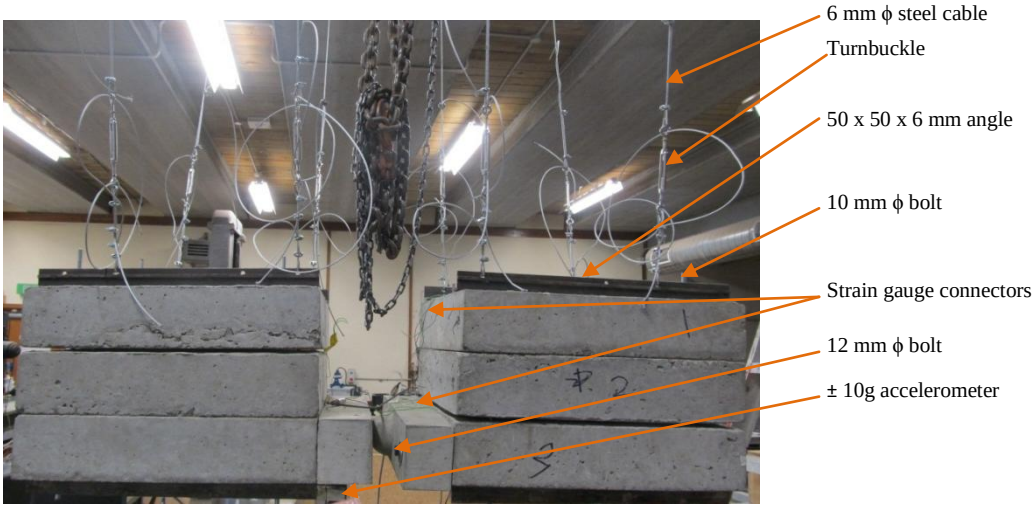

Fig. 3 Pounding with three concrete slabs on each pendulum (case s3-i3)

Table 2 Slab combination

Case*	No. of slabs in pendulum		Striker mass (kg)	Struck mass (kg)
	Striker	Struck		
s1-i1		single	109	108
s1-i2	Single	double	109	199
s1-i3		triple	109	290
s2-i1		single	200	108
s2-i2	Double	double	200	199
s2-i3		triple	200	290
s3-i1		single	291	108
s3-i2	triple	double	291	199
s3-i3		triple	291	290

*In case sj-ij, s and i denote the striker slab and the impacted slab, respectively and j is the number of slabs

slab configurations. However, no vertical in-plane rotation was visible due to this eccentricity, because the impact velocities and the pounding force are small.

Each pendulum had a ± 10 g accelerometer attached to the bottom face of the slab, under the centre of the impacting side. The accelerometers have a frequency range from 0.3 Hz to 10 kHz. The displacement of the slabs was measured by a laser sensor focused on the opposite (non-impacting) end of the slab. The sensors have a precision of 0.3 mm. They are not sensitive enough to measure the impact-induced relative displacement. The slab velocities are calculated from expressions for motion of a simple pendulum. An attempt was made to measure pounding force from strain gauges affixed to the reinforcement nets of the slab. However, the strain gauge results were below the noise threshold in the case of the impact velocities considered.

The impact was initiated by displacing the right mass (Fig. 1) and allowing it to swing back and strike the left slab. Henceforth, the displaced slab is called striker slab and the second slab is called struck slab. Both masses move after the first impact and multiple impacts occur as they swing back

and forth. The results were discarded if out-of-plane motion, i.e. twisting motion of the slabs, was observed after the first impact. With spherical contact element, 6-7 full cycles of twists occurred in the time required to complete a half cycle of swinging motion between two subsequent impacts. However, the masses always showed out-of-plane motion after second or third impact. Since only the first impact was considered and processed in the results, the out-of-plane movement resulting from subsequent impacts has no relevance. Additionally, simultaneous full contact at the initiation of impact could not be achieved for cylindrical and plane contact surfaces, resulting in large out-of-plane motion even after the first impact. Thus, most of the tests were conducted only for the 100 mm ϕ hemispherical attachments. For comparison, some impacts were conducted for the case s1-i1 with the other pounding elements shown in Table 1, despite the presence of out-of-plane movement.

The initial displacement, *d* of the striker was between 1 and 7 cm. At the beginning of tests with each impact element, a few unrecorded impacts were conducted at *d* = 7 to 9 cm so as to remove asperities at the contact interface. This ensured repeatability of the test because otherwise the stiffness of the contact element may change at higher impact velocities due to damage accumulation. The hemispherical contact heads were slightly flattened (approx. 0.5 - 1 mm) ue to these initial high velocity impacts while no effect was seen in cylindrical and plane contact surfaces. No other permanent deformations were observed until the completion of the tests.

3. Results and discussion

The displacement and acceleration time-histories for case s1-i1, when the striker slab with the 100 mm diameter hemispherical element was displaced 58 mm, are shown in Fig. 6. The displacement shows two phases: (i) the period when the striker was displaced and stabilized

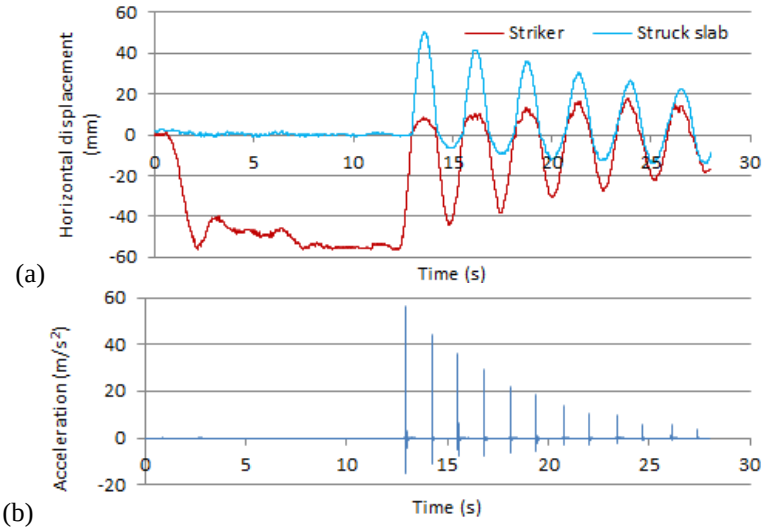

Fig. 4 Time history of (a) displacement of the slabs and (b) acceleration of the striker, initial displacement of the striker, *d* = 58 mm

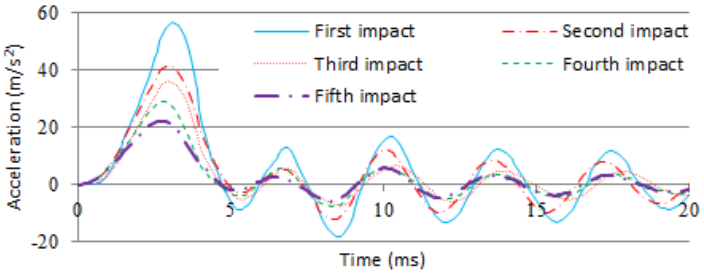

Fig. 5 Impact accelerations for the first five impacts in Fig. 6

at 58 mm displacement and (ii) the period when the striker was released and impacts and subsequent separations occurred. The velocity of the striker before the first impact was calculated to be 0.145 m/s. The immediate post-impact velocities of the striker and the struck slabs were 0.02 m/s and 0.126 m/s, respectively. The coefficient of restitution was 0.73. The largest acceleration magnitude of subsequent impacts decreased with each impact (Fig. 6(b)). As anticipated the reduction in magnitude is due to decreasing impact velocity.

The accelerations show a surprisingly high negative component (approx. 1.85 g). As shown in Fig. 7, the acceleration due to five successive impacts in the same test show minimal phase shift. The periodicity of the acceleration reflects a characteristic of impact-induced standing wave in the slabs.

3.1 Effect of mass variation

Fig. 8 shows the effect of equal change in both masses. The coefficient of restitution decreased with the increasing mass. For the case with equal slabs e.g. case s1-i1, *e* varies slightly with the impact velocity but there is no particular trend. For the impact of single slabs, *e* increases with

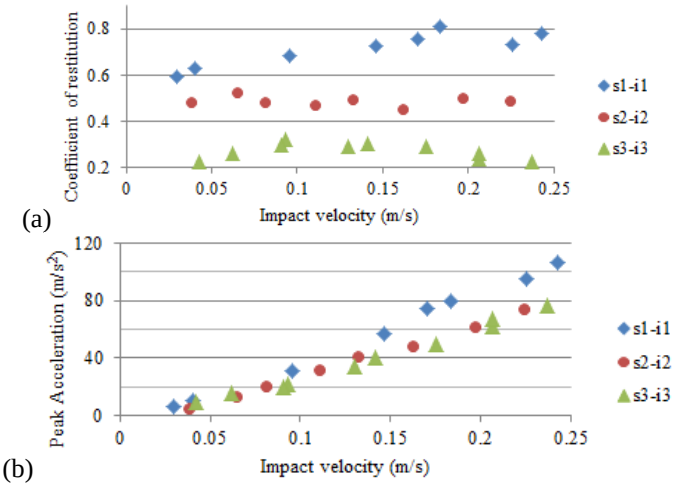

Fig. 6 Effect on (a) coefficient of restitution and (b) peak impact acceleration, due to equal change in the mass of both pendulums

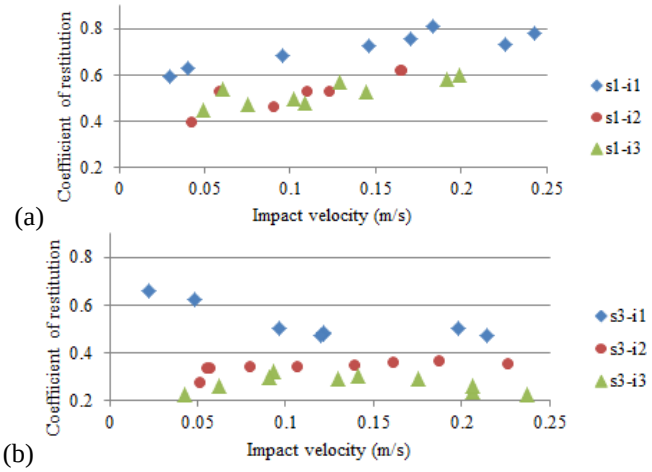

Fig. 7 Variation in coefficient of restitution for three different masses of struck slab when striker has (a) only one slab and (b) three slabs

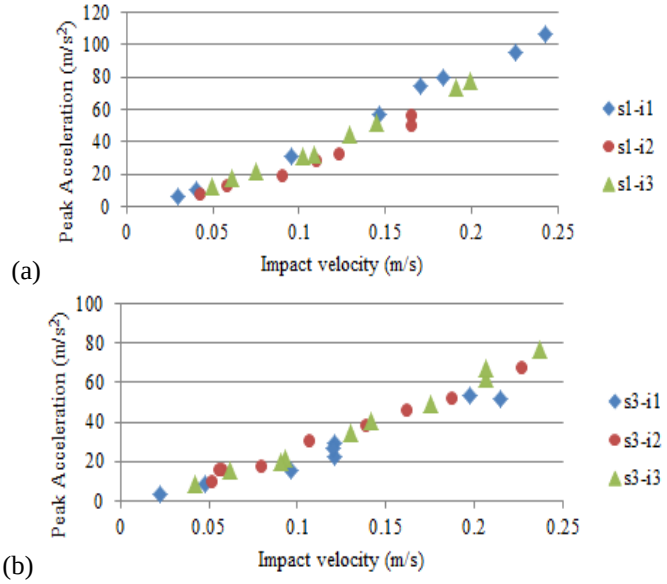

Fig. 8 Peak impact acceleration under various mass and velocity combinations for strikers with (a) a single slab and (b) three slabs

velocity. For the heaviest masses, i.e. case s3-i3, *e* increased up to 0.1 m/s impact velocity, remained almost constant between 0.1 to 0.15 m/s and thereafter decreased. For case s2-i2 no significant variations is observed. As anticipated, the peak acceleration magnitude is almost linearly proportional to the velocity in all three cases.

The effect of unequal variation in mass on coefficient of restitution is presented in Fig. 9. The striker is kept constant and the mass of the struck pendulum is varied. The results are shown for (i) the lightest striker i.e. one slab and (ii) the heaviest striker *i.e.* three slabs. In both cases, *e* decreased as the mass of the struck pendulum increased. For the lightest striker there is an

increasing trend with higher velocity for all three mass combinations. For the heaviest striker an increase in impact velocity either had no effect or produced a smaller *e*. A comparison between case s1-i3 (Fig. 9(a)) and case s3-i1 (Fig. 9(b)) shows very different values for *e*. Thus, *e* is affected not only by the total mass of the system but also by the ratio of the striker and the struck mass.

Similar to the case of equal masses, the peak acceleration in unequal masses shows almost linear relationship with impact velocity and appears independent of participating masses (Fig. 10).

3.2 Effect of change in contact surface

Substantial out-of-plane motion was observed when the cylindrical and plane contact elements were used. The cylindrical and plane elements produce a line and area contact, respectively, while the spherical element produces a point contact. An instantaneous full contact cannot be achieved even with very careful preparation and execution; the contact develops over time and causes out-of-plane movement. The coefficient of restitution with cylindrical and plane contact elements was significantly smaller (Fig. 11(a)) compared to that with spherical contact element. For low impact velocities the plane element produced only one impact. The pendulums then moved together. The coefficient of restitution and peak impact acceleration (Fig. 11(b)) increased with velocity all three surfaces.

The first acceleration pulse obtained with the three contact elements for the case s1-i1, at approximately 0.15 m/s impact velocity, is shown in Fig. 12. The acceleration from spherical contact shows smooth lines while some small deviations are seen in cylindrical contacts. The acceleration obtained with plane contact surface has clearly visible discontinuities. Thus, the results establish that the details of the geometry of the contact surface play a significant role in the development of impact-induced response.

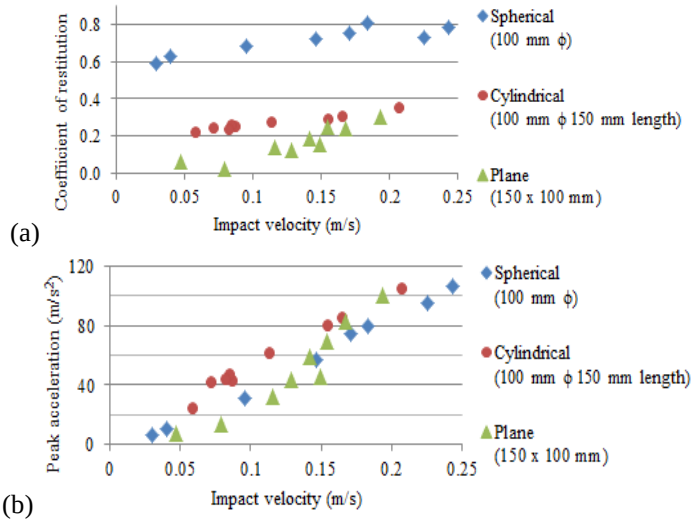

Fig. 9 Effect of contact interfaces, in the case s1-i1, on (a) coefficient of restitution and (b) peak impact acceleration

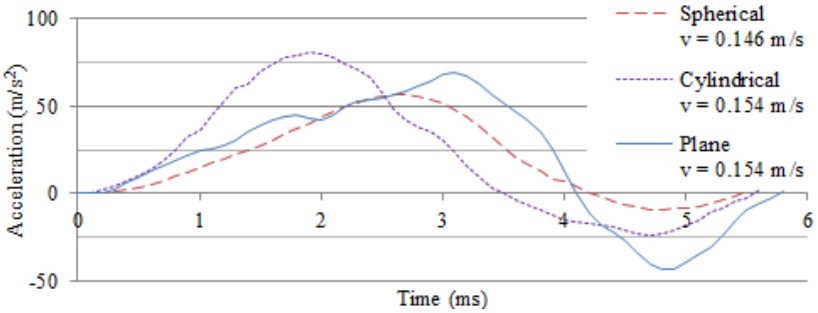

Fig. 12 Influence of the impact interface on the response

4. Comparison with numerical force models

The existing numerical force models for pounding simulation can be classified into (i) lumped-mass models and (ii) distributed-mass models.

4.1 Lumped-mass models

These models consider colliding bodies as concentrated masses and the pounding force is simulated by a viscoelastic link inserted between them. The link is placed in series with a gap element such that compressive force is generated when the gap closes and no force exists when the gap is open (Anagnostopoulos 1988). The energy loss during impact is represented by damping of the link, which is calculated from the coefficient of restitution. The lumped-mass models can be further subdivided into (a) linear and (b) nonlinear contact elements. The pounding force is calculated as $F = k\,\delta^n + c\delta^p\,\delta`$, where $k$ is the linear or nonlinear impact stiffness, $c$ is a constant dependent on the coefficient of restitution $e$, $\delta$ is the apparent deformation and $\delta`$ is the instantaneous relative velocity. n equals 1 for linear elements (Anagnostopoulos 1988, Mahmoud and Jankowski 2011, Khatiwada *et al*. 2014) and 3/2 for nonlinear elements based on Hertz contact law (Jankowski 2005, Khatiwada *et al*. 2014). The value of p varies according to the model used. The detailed descriptions and individual equations for the various models can be found elsewhere (e.g. Khatiwada and Chouw 2014).

A major weakness of lumped-mass models is the lack of an analytical expression to calculate k from material and geometrical properties of the pounding masses. Although the Hertz contact law contains a formula for k, it has been demonstrated that the stiffness calculated is not applicable to inelastic contacts (Goldsmith 2001, van Mier *et al*. 1991). Consequently, k is often retroactively estimated from experimentally recorded responses (Jankowski 2005, Guo *et al*. 2012).

Fig. 13 compares the experimental peak accelerations for all velocities in case s1-i1 against those calculated from four numerical models, *viz*. linear viscoelastic model (LVE, Anagnostopoulos 1988), linear Hunt-Crossley model (LHC, Khatiwada *et al*. 2014), nonlinear viscoelastic model (NlVe, Jankowski 2005) and corrected Hertzdamp model (Hd, Khatiwada *et al*. 2014). The k for the numerical models (Table 3) were estimated by equating the numerical and experimental peak accelerations for v = 0.145 m/s. The damping c for each impact is obtained from the coefficient e calculated from the experimental results. Both experimental and numerical peak accelerations in Fig. 13 increase almost linearly with velocity. There is a good agreement

between the numerical and experimental results. However, the two sets of results differ when mass is varied (Fig. 14). The numerical peak acceleration of the striker increases with the mass of the struck slab while the experimental accelerations show a very small change.

Three significant limitations of lumped-mass models have been identified from comparison with the experimental results: (i) the lumped-mass models only produce one half-cycle of the impact acceleration (Jankowski 2005, Khatiwada *et al*. 2014) and they cannot predict the oscillations observed after the first peak in the experimental results (see Fig. 7), (ii) coefficient of restitution, a critical parameter for all lumped-mass models, shows substantial variation with no general trend when the mass of pounding slabs as well as the ratio of the participating mass is changed, (iii) the contact stiffness cannot be predicted analytically and seems to vary when the mass of the pendulums is changed in contrast to the assumptions of the lumped-mass models that it is only affected by the material and geometrical properties of the contact interface.

Table 3 Stiffness *k* for lumped-mass models

Model	Stiffness
LVe	41.8 MN/m
LHC	35.8 MN/m
NLVe	3.47 GN/m$^{3/2}$
Hd	2.13 GN/m$^{3/2}$

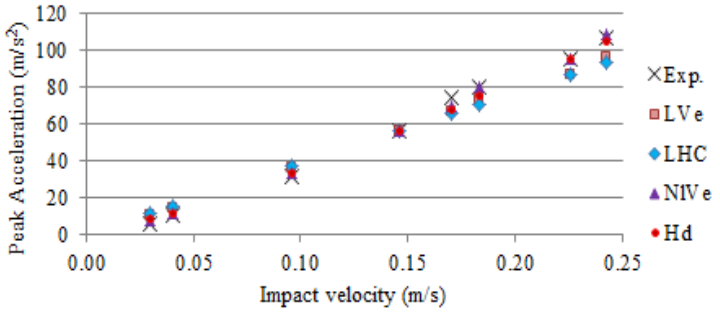

Fig. 10 Experimental and simulated peak accelerations for case s1-i1 with hemispherical contact element

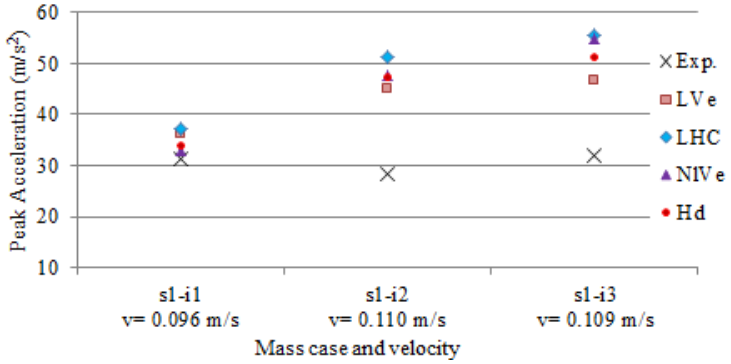

Fig. 11 Influence of mass configuration on experimental and numerical peak acceleration

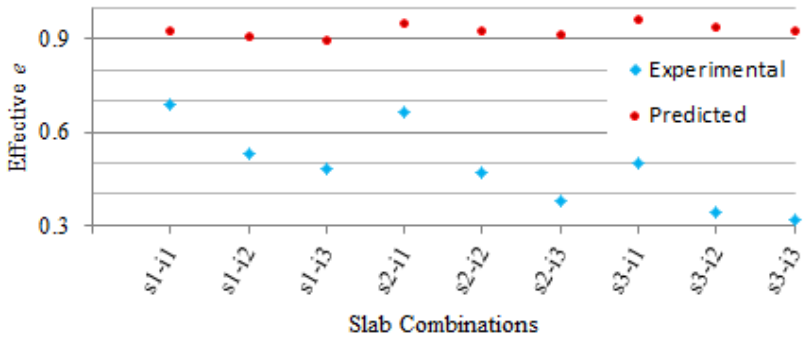

Fig. 12 Comparison of eeff predicted by the distributed-mass models and e calculated from experiments

4.2 Distributed-mass models

These models consider the mass of the colliding slabs to be distributed over their length. The pounding force is calculated from the wave theory of impact (Goldsmith 2001, Graff 1991) which assumes that an impact generates compressive stresses at the contact interface which propagate away from contact towards the far ends of the slabs. When these waves arrive at the far ends, they get reflected back toward the contacting ends. Separation occurs when one of the reflected waves reaches the contact location (Cole *et al*. 2011). Details of these models can be found in Khatiwada and Chouw (2014).

The distributed-mass models do not require a value of coefficient of restitution for simulation of impact. The pounding force has a constant magnitude throughout the contact duration. This magnitude depends only on the impact velocity and the material and geometrical properties of the slabs. The contact duration is the time taken by the stress waves to travel twice through the shorter slab, i.e. from the contact location to the far end, and back to the contact location. The effective coefficient of restitution, e_{eff}, can be calculated as the ratio of calculated relative velocities after impact to the relative velocity prior to impact. For the impact of slabs of identical material and cross-sections, e_{eff} equals the ratio of the length of the shorter slab to the longer slab. For slabs of different cross-sections, the formula for e_{eff} is given by Cole *et al*. (2011). The calculated e_{eff} for the nine cases considered in this study are shown in Fig. 15. It is apparent that in all cases the predicted e_{eff} is substantially higher than that calculated from the experimental results. The distributed-mass models fail to predict the variation in e with changes in the impact velocity because the expression for effective e is independent of the impact velocity (Cole *et al*. 2011, Malhotra 1998). From the material properties of the bars, the stress waves should require 0.473 ms and 0.439 ms to travel twice through the striker and the struck slabs respectively. However, the first acceleration pulse alone lasts almost 5 ms (see Fig. 7).

5. Conclusions

A series of impacts between reinforced concrete slabs as pendulums was conducted. A parametric investigation of coefficient of restitution and impact-induced peak acceleration was carried out by varying the velocities, pendulum masses and the contact surface geometry. A total

of 95 impacts were performed.

The investigation reveals:

- The coefficient of restitution was influenced by the total mass of the striker and the struck pendulums, striker mass and the ratio of the masses. The coefficient decreased with increasing total mass.
- For similar impact velocity, the coefficient increased with a heavier striker mass; and decreased in the case of lighter striker impacting a heavier pendulum.
- With increasing impact velocity the coefficient of restitution did not show any general trend. For an impact of equal masses, the coefficient increased with velocity for the lightest mass considered. However, for heavier mass this is not the case. The coefficient also increased with velocity when a lighter mass struck a heavier mass, and decreased with velocity when the striker was heavier.
- The peak acceleration increased almost linearly with impact velocity and was almost insensitive to the striker, struck and total mass.
- The geometry of the impact element plays a significant role in the development of impact-induced peak accelerations.
- The experimental accelerations cannot be predicted by either the lumped-mass or distributed-mass models of pounding. Although the lumped-mass model produced a consistently close prediction of pounding-induced accelerations in the impact between single slabs, the acceleration of multiple-slabs could not be simulated. The distributed-mass models predict almost elastic impacts for the slabs used in these experiments while the experimental results involve considerable energy loss. The results suggest that a refinement of the current numerical force models is required before they can be used for design purposes.

The results of the experiments conducted in this study show for the first time that the coefficient of restitution, defined in conventional impact between two particle masses, cannot be applied in impact between components of structures. This is because the definition of the coefficient of restitution is based solely on velocities of participating masses without considering the distribution of masses, damping and stiffness along the structural members as well as structural boundary conditions.

Acknowledgments

The authors gratefully acknowledge the University of Auckland International Doctoral Scholarship awarded to the first author.

References

Anagnostopoulos, S.A. (1988), "Pounding of buildings in series during earthquakes", *Earthq. Eng. Struct. Dyn.*, **16**(3), 443-456.

Athanassiadou, C.J., Penelis, G.G. and Kappos, A.J. (1994), "Seismic response of adjacent buildings with similar or different dynamic characteristics", *Earthq. Spect.*, **10**(2), 293-317.

Bothara, J.K., Jury, R.D., Wheeler, K. and Stevens, C. (2008). "Seismic assessment of buildings in Wellington: experiences and challenges", *Proceedings of the 14th World Conference on Earthquake*

Engineering, Beijing, October.
Chouw, N. (2002), "Influence of soil-structure interaction on pounding response of adjacent buildings due to near-source earthquakes", *JSCE J. Appl. Mech.*, **5**, 543-553.
Chouw, N. and Hao, H. (2008), "Significance of SSI and nonuniform near-fault ground motions in bridge response I: Effect on response with conventional expansion joint", *Eng. Struct.*, **30**(1), 141-153.
Chouw, N. and Hao, H. (2012), "Pounding damage to buildings and bridges in the 22 February 2011 Christchurch earthquake", *Int. J. Protect. Struct.*, **3**(2), 123-140.
Cole, G.L., Dhakal, R.P., Carr, A. and Bull, D. (2010), "Building pounding state of the art: Identifying structures vulnerable to pounding damage", *New Zealand Society for Earthquake Engineering Annual Conference*, Wellington, April.
Cole, G.L., Dhakal, R.P., Carr, A. and Bull, D. (2011), "An investigation of the effects of mass distribution on pounding structures", *Earthq. Eng. Struct. Dyn.*, **40**(6), 641-659.
Goldsmith, W. (2001), *Impact: the theory and physical behaviour of colliding solids*, Dover Publications, New York, USA.
Guo, A., Cui, L. and Li, H. (2012), "Impact stiffness of the contact-element models for the pounding analysis of highway bridges: Experimental evaluation", *J. Earthq. Eng.*, **16**(8), 1132-1160.
Guo, A., Li, Z., Li, H. and Ou, J. (2009), "Experimental and analytical study on pounding reduction of base-isolated highway bridges using MR dampers", *Earthq. Eng. Struct. Dyn.*, **38**(11), 1307-1333.
Graff, K. (1991), *Wave motion in elastic solids*, Dover Publications, New York, USA.
EERI special earthquake report (2001), "Learning from earthquakes: preliminary observations on the origin and effects of the January 26, 2001 Bhuj (Gujarat, India) earthquake", Oakland, California, USA.
Khatiwada, S. and Chouw, N. (2014), "Limitations in simulation of building pounding in earthquakes", *Int. J. Protect. Struct.*, **5**(2), 123-150.
Khatiwada, S., Chouw, N. and Butterworth, J.W. (2014), "A generic structural pounding model using numerically exact displacement proportional damping", *Eng. Struct.*, **62-63**, 33-41.
Jankowski, R. (2005), "Nonlinear viscoelastic modelling of earthquake induced structural pounding", *Earthq. Eng. Struct. Dyn.*, **34**(6), 595-611.
Jankowski, R. (2007), "Theoretical and experimental assessment of parameters for the non-linear viscoelastic model of structural pounding", *J. Theoret. Appl. Mech.*, **45**(4), 931-942.
Jankowski, R. (2010), "Experimental study on earthquake-induced pounding between structural elements made of different building materials", *Earthq. Eng. Struct. Dyn.*, **39**(3), 343-354.
Jeng, V. and Tzeng, W. (2000), "Assessment of seismic pounding hazard for Taipei city", *Eng. Struct.*, **22**(5), 459-471.
Kasai, K. and Maison, B.F. (1997), "Building pounding damage during the 1989 Loma Prieta earthquake", *Eng. Struct.*, **19**(3), 195-207.
Leibovich, E., Rutenberg, A. and Yankelevsky, D.Z. (2012), "Pounding response of adjacent concrete rods: an experimental study", *Int. J. Protect. Struct.*, **3**(3), 355-374.
Leibovich, E., Yankelevsky, D.Z. and Rutenberg, A. (1994), "Pounding response of adjacent concrete slabs: an experimental study", *Proceedings of the 17th Regional European Seminar on Earthquake Engineering*, Haifa, Israel, September.
Li, B., Bi, K., Chouw, N., Butterworth, J.W. and Hao, H. (2012), "Experimental investigation of spatially varying effect of ground motions on bridge pounding", *Earthq. Eng. Struct. Dyn.*, **41**(14), 1959-1976.
Li, B., Bi, K., Chouw, N., Butterworth, J.W. and Hao, H. (2013), "Effect of abutment excitation on bridge pounding", *Eng. Struct.*, **54**57-68.
Mahmoud, S. and Jankowski, R. (2011), "Modified linear viscoelastic model of earthquake-induced structural pounding", *Iranian J Sci. Tech. Trans. B- Eng.*, **35**(C1), 51-62.
Malhotra, P. (1998), "Dynamics of seismic pounding at expansion joints of concrete bridges", *ASCE J. Eng. Mech.*, **124**(7), 794-802.
Masroor, A. and Mosqueda, G. (2012a), "Experimental and numerical Simulation of limit states in base isolated buildings including pounding", *20th Analysis and Computation Specialty Conference*, Chicago,

March.
Masroor, A. and Mosqueda, G. (2012b), "Experimental simulation of base-isolated buildings pounding against moat wall and effects on superstructure response", *Earthq. Eng. Struct. Dyn.*, **41**(14), 2093-2109.
Muthukumar, S. and Des Roches, R. (2006), "A Hertz contact model with non linear damping for pounding simulation", *Earthq. Eng. Struct. Dyn.*, **35**(7), 811-828.
Papadrakakis, M. and Mouzakis, H.P. (1995), "Earthquake simulator testing of pounding between adjacent buildings", *Earthq. Eng. Struct. Dyn.*, **24**(6), 811-834.
Rosenblueth, E. and Meli, R. (1986), "The 1985 earthquake: causes and effects in Mexico city", *Concrete Int.*, **8**(5), 23-34.
Bureau of Indian Standards (2000), *IS 456*, Plain and reinforced concrete code of practice, India.
Van Mier, J., Pruijssers, A., Reinhardt, H. and Monnier, T. (1991), "Load time response of colliding concrete bodies", *J. Struct. Eng.*, **117**(2), 354-374.
Zhu, P., Abe, M. and Fujino, Y. (2002), "Modelling three dimensional non linear seismic performance of elevated bridges with emphasis on pounding of girders", *Earthq. Eng. Struct. Dyn.*, **31**(11), 1891-1913.

IT